Computers and Electrical Engineering 101 (2022) 108094

Contents lists available at ScienceDirect

Computers and Electrical Engineering

journal homepage: www.elsevier.com/locate/compeleceng

Artificial neural network-based cardiovascular disease prediction using spectral features☆

Misha Urooj Khan [a], Sana Samer [a], Mohammad Dahman Alshehri [b], Naveed Khan Baloch [c], Hareem Khan [c], Fawad Hussain [c], Sung Won Kim [d], Yousaf Bin Zikria [d,*]

[a] Department of Electronics Engineering, University of Engineering and Technology, Taxila, 47080, Pakistan
[b] Department of Computer Science, College of Computers and Information Technology, Taif University, Taif, 21944, Saudi Arabia
[c] Department of Computer Engineering, University of Engineering and Technology, Taxila, 47080, Pakistan
[d] Department of Information and Communication Engineering, Yeungnam University, Gyeongsan, 38541, South Korea

ARTICLE INFO

Keywords:
Cardiovascular disease
Machine learning
Heart murmur
Phonocardiogram
Spectral analysis
Artificial neural network
Classification
Segmentation
Minimum redundancy maximum relevance
Feature analysis

ABSTRACT

The major cause of the increasing world mortality rate is cardiovascular disease (CVD), killing 17.9 million people annually. Current techniques are costly, challenging to operate on, and an expert is needed to confirm the diagnosis results. Phonocardiogram (PCG) signals are heart sound recordings of heart rhythms and have many advantages over traditional auscultation methods. This work targets CVD detection through PCG signal analysis using different artificial neural networks (ANN) and fusion of spectral features. PCG signal is acquired through the subject's heart by a self-designed PCG acquisition setup. It is then pre-processed and extracted five spectral features with the highest pair-wise differences. Five different types of ANN named narrow, wide, tri-layered, bi-layered, and medium are simulated with 99.99% accuracy. This proposed architecture is non-invasive, moderate, and reliable compared to current approaches and also offers great guidance in offering new low-cost alternatives for CVD diagnosis techniques.

1. Introduction

Cardiovascular disease is the world's leading cause of death which claims the lives of 17.9 million people globally each year. That is why the development of electronic instruments that can help the early detection of these diseases is a hot topic. It is common to use the electrocardiogram (ECG) technique, but some of the diseases can be detected by heart sound auscultation. As our heart is pumping continuously, the signals produced by the heart are traveling at a faster rate and are very complex in nature. A heart may produce four sounds during a single cycle named S1 (lub sound) and S2 (dub sound), while S3 and S4 are quite rare. S1 is caused by the atrioventricular valve closure and S2 by the closure of semilunar valves. S3 and S4 are less common heart sound that cannot be heard but can be seen on a visual recording, such as a phonocardiogram. The cardiac cycle is the time it takes from the start of one heartbeat to the beginning of the next. The time cycle of S1 and S2 is used to identify abnormal sounds, while their amplitudes provide information about cardiac wall contraction and expansion. Heartbeats at an incredibly steady rate of 60 to 100 beats per minute, or 100 thousand times a day. When the heart beats irregularly or abnormally, doctors refer to it as abnormal pulse and

☆ This paper is for special section VSI-aihc. Reviews were processed by Guest Editor Dr. Deepak Gupta and recommended for publication.

* Corresponding author.
E-mail addresses: yousafbinzikria@ynu.ac.kr, yousafbinzikria@gmail.com (Y.B. Zikria).

https://doi.org/10.1016/j.compeleceng.2022.108094
Received 2 January 2022; Received in revised form 5 May 2022; Accepted 16 May 2022

cardiac arrhythmia. It causes abrupt pulse murmurs that are either too slow or too fast. Strokes occur when the heart slows or stops blood flow to the brain. As a result, the nutrients that your brain requires are unavailable, and thus brain cells start dying. Human body cannot function normally if its blood cannot enter the exact output portion or body part. A blocked artery or unexpected bursts cause a stroke. It needs to be treated as soon as possible to avoid any brain injury and other risks. Coronary artery disease (CAD) occurs when the veins that supply essential components and resources to the heart stiffen. This hardening is also known as arterial sclerosis. Blood clots in major arteries, usually in the legs, are caused by deep vein deformation and infarction. Electrical activation occurs first in the cardiac cycle, followed by mechanical activity in the form of atrial and ventricular movements. As a result, blood flows between the heart chambers and throughout the body, opening and closing the heart valves. The mechanical activity of the heart, as well as the sudden starting or termination of blood flow, causes the whole cardiac structure to vibrate. These tremors are heard on the thoracic wall and can indicate the health of the heart. The recording of these rhythms is known as PCG. The PCG signals detect significant information related to heart health and are a crucial technique for distinguishing various heart diseases. The frequency of normal heart sound is low compared to the heart murmurs which have a high frequency. Heart murmurs (HMs) are usually created due to the narrowing and blockage of heart walls. It may also be due to the faster blood pumping than the normal rate. HMs can be present in newborns or present in older people due to aging. It can be classified into normal and abnormal. An abnormal murmur (AM) causes severe heart diseases, but the normal one is not causing any risk or harm. In adults, AM is most commonly caused heart valve issues such as valve thickness, Endocarditis, or Rheumatic fever. It is caused by structural cardiac abnormalities named congenital heart defects in children, which include holes in the heart, cardiac shunts, and heart valve issues present from birth. There are no significant symptoms of a normal murmur, but an abnormal murmur causes blue lips and fingertips, cough, chest pain, and liver enlargement.

Heart auscultation is a technique used by clinicians to examine cardiovascular functioning and diagnose abnormalities, but their analysis takes a long time. As a result, deep learning techniques may play a critical part in understanding these signals so that physicians can make corrective decisions for the detected disorder. As a result, modern technologies are necessary to improve lifestyle and health care. More specifically, extensive research undertaken in partnership with researchers, health care providers, and patients is essential for establishing accurate and tailored treatment choices for a wide range of illnesses. Electronic stethoscopes utilize filtering and amplification to increase the clarity of body sounds. If a deep learning-based diagnosis of the heart can improve precision and productivity, we can save expenditure on healthcare while also improving quality.

1.1. Problem statement

PCG technique is one of the most emerging and used techniques for cardio diseases in recent ages. Almost all previous studies focused only on developing cardiac abnormality detection algorithms. Still, very few dealt with developing a low-cost, portable, easy to operate PCG acquisition system (PAS) that could be installed in a healthcare environment. PCG signals are digital cardiac sounds that give vital insights for remote patient monitoring and intelligent diagnosis in a non-invasive manner using multiple signal processing and artificial intelligence techniques. As a result, a thorough assessment is required to design a PCG acquisition system with a robust algorithm for detecting CVDs from most conventional heart sounds.

This research aims to build a standalone sensor to detect low-frequency PCG signals using this self-designed system formation of a database containing PCG signals from different heart pathologies and healthy subjects. In the first phase, we designed the PAS, tested it various times, and gave it a portable shape after satisfying good results. The second phase included the collection of heart sounds. The third phase was to get them annotated by medical experts. The fourth phase was the development of an algorithm for immediate pathological detection and classification in real-time.

Following are the primary contributions of this research study:

i. Developed a low-cost PCG acquisition system (PAS) named DS-101 designed to record different heart sounds from local subjects/patients.
ii. Collection of normal and abnormal PCG signals from consented patients and subjects.
iii. Annotation of the dataset by competent clinical experts/cardiologists using standard auscultation.
iv. Data training on five different types of artificial neural networks with best spectral features having maximum class wise difference.
v. Deployment of less extensive computational algorithm with robust detection and classification of CVD's.
vi. Comprehensive experimental results with excellent classification metrics confirmed the superiority of the proposed algorithm over the state-of-the-art methods.

The remainder of the article is arranged in the following manner: Section 2 state of art-related work. Section 3 provides an overview of the architecture of self-designed digital stethoscopes. Section 4 explains the methodology. Section 5 provides detailed results and discussion. Finally, Section 6 concludes the paper with future work.

2. Related work

Digital subtraction phonocardiography (DSP) is used to separate heart murmurs from normal PCG signals. The recordings were obtained from 60 infants. DSP can be a dependable and cost-effective breakthrough diagnostic method for testing for structural heart disease. Still, it has to be tested on a large number of patients with well-defined pathophysiology to establish its clinical potential [1]. Sundaram et al. applied the multiscale entropy (MSE) technique and Mann–Whitney test to discriminate between normal PCG and

Fig. 1. Block diagram of self-designed PCG Acquisition System (PAS).

artifact sound signals. The MSE of normal and artifact signals was substantially different when a value of $P < 0.01$ was used. However, to validate this approach, a significant amount of data set must be available with balanced class samples [2]. Systolic and pathological murmurs were distinguished using color spectrographic phonocardiography by Sarbandi et al. The source of the continuous low-frequency energy observed in several recordings is unknown due to poor skin contact of the chest piece. To make this technique more effective, investigations on many individuals with homogeneous cardiac abnormalities are also required [3]. Classification of heart sound signals is done using Wavelet decomposition, autoregressive (AR) model, and normalized Shannon energy with an accuracy of 93%. Misclassification is caused by several significant interferences such as speaking, wailing, or other noises. The abrupt removal of the stethoscope from the patient's chest for a brief period during data collection also resulted in an inaccurate diagnosis. Better recording techniques can improve the misclassification, recordings and protocols [4]. Huiying et al. generated frequency envelopes of the PCG signal using Discrete wavelet analysis. Large intensity murmurs overlapping with Sl or S2 were difficult to separate but can be differentiated by critically evaluating spectrogram generation or monitoring the PCG signal. [5].

It is worth mentioning that the thresholds for heart sound classification change strongly with different data types, but He et al. strengthened this by adding new methods for S2 feature extraction as he applied automatic heart sound segmentation with 74% accuracy. [6]. Gill et al. proposed heart sound detection using homomorphic filtering (HF) and computed tomography (CT) to extract a smooth envelogram. The addition of supervised learning can further improve this algorithm, and time–frequency characteristics for the identification of additional heart sound such as S3, S4, murmurs, and valve abnormalities [7]. Misha et al. proposed an efficient algorithm for classifying normal and extrahls PCG signals. They used empirical mode decomposition (EMD) for noise reduction, soft thresholding for signal segmentation, impulsive domain features, and multiple ensemble-based classifiers. It achieved 98.8% accuracy, but its dataset is only 400 samples, with each signal duration only up to 10 s. As the signal duration used by them is small, they must increase the number of samples so that it can be generalized [8]. Choi et al. used AR spectral analysis and multi support vector machine (SVM) to characterize cardiac sound murmurs efficiently. If the SVM module is constructed with a specified threshold value (THV), then only this technique can show good classification performance [9]. Multi-class heart sound detection and classification are done using 2D-convolutional neural networks (CNN). The suggested model has an overall test accuracy of 83%, which is relatively low compared to others in literature [10]. Babaei et al. cleaned PCG data with the daubechies wavelet, retrieved statistical features for three cardiac valve problems, and trained ANN with a 94.42% accuracy [11]. Ahmed et al. collected datasets with a Littman 3200 electronic stethoscope and extracted normalized average Shannon energy and 50 mel-frequency cepstrum coefficients (MFCCs). By training extracted features on medium gaussian SVM, a classification accuracy of 92.6% was attained [12].

The goal of all of the above methods is to categorize cardiac disease. But it contains the following limitations, (i) limited dataset, (ii) threshold calculated for one dataset does not work well for other datasets containing different diseases, (iii) the stethoscopes used for recording has poor skin contact, which results in PCG signals with missing vital information (iv) recorded sounds have large intensity and overlapping characteristics (v) High priced digital stethoscopes cannot be afforded by everyone and (vi) the available online datasets have a significant amount of class imbalance. This is why the deployment of accurate algorithms capable of diagnosing a wide range of cardiac problems based on good quality PCG signals has become crucial. The key challenges in developing appropriate algorithms are the large diversity of heart sounds and the non-stationary nature of PCG signals. With these challenges, the question of how to increase the distinctiveness of audible heart sounds and improve the effectiveness of such algorithms while reducing computational costs without sacrificing reliability must be considered. Therefore, in this work, we used a low-cost self-developed PAS with an efficient algorithm for classifying CVDs with high accuracy, sensitivity, and specificity. The collected dataset contains 2310 Normal and 2300 abnormal PCG signals with almost no class imbalance between them. All recorded sounds are of high quality, which can later be used for training medical students. A time-domain signal is converted into a frequency-domain signal using spectral features. It uncovers signal qualities that are not time-local but are stretched over the periods. It unhides all the crucial information that was previously concealed and gives fine-grained information with low-frequency resolution. Neural networks are considered the most effective technique for predicting heart and brain disease. Therefore, the proposed system use classifier with spectral features having a significant class difference. The achieved results indicate an improved degree of effectiveness compared to previously employed techniques in the literature.

Table 1 summarizes the literature review and compares the types of datasets used, focused diseases, extracted features, classifiers, and achieved results with classification parameters named accuracy (ACC), sensitivity (SN), and specificity (SP).

Table 1
Comparison of previous studies.

Research	Recording's/Dataset	Diseases/Types of PCG signals	Features and methods	Results
[1]	60 infants and adults	Heart murmur	Digital subtraction Phonocardiography (DSP) Murmurgram	Separation of cardiac murmurs
[2]	Peter bentley heart sounds database 10 samples of normal and artifact signal	Cardiac valve disorders	Multiscale entropy technique Mann–Whitney test	Discrimination of normal and artifact PCG signal
[3]	Self-collected dataset Normal cases: 5 Patients: 45	Cardiac abnormalities	Not provided (NP) Color spectrographic analysis	Identification of cardiac conditions
[4]	Self-collected dataset Pathological murmurs: 14 Physiological murmur: 23	Heart sounds	Normalized average Shannon energy Automatic segmentation algorithm	Decision of durations of S1 and S2
[5]	Self-collected dataset 77 recordings	Normal and abnormal heart sounds	Normalized average Shannon energy Identification of S1 and S2	93% correct segmentation ratio
[6]	Not provided	Classification of heart sound signals	Wavelet decomposition (coif5) Normalized average Shannon energy Aortic valve closure (A2) as a feature of S2	SP: 61% SN: 87% ACC: 74%
[7]	44 phonocardiograms	Heart sound	Homomorphic envelogram Baum–Welch algorithm Hidden Markov model	S1:98.61% specificity S2: 98.3% specificity
[8]	Self-collected dataset Normal: 200 samples Extrahls: 200 samples	Normal and Extrahls PCG signals	Impulsive domain features K-Nearest Neighbors (KNN)	ACC: 98.8%
[10]	PASCAL dataset	Multi-class heart sounds classification	MFCC 2D-CNN	ACC: 83%
[11]	Not provided	Heart valve disorders	Daubechies wavelet filter Statistical classifier ANN	ACC: 94.42%
[12]	283 sound samples	Classification of cardiovascular disorder	MFCC SVM KNN	ACC: 92.6%

3. PCG acquistion system

3.1. Existing databases

The University of Michigan Health System supplied the michigan heart sound and murmur database (MHSDB) [13]. It contains 23 cardiac sound recordings with a total length of 1496.8 s, while the PASCAL [14] database contains 656 recordings for heart sound classification and 176 recordings for heart sound segmentation. The recording quantity, duration, and signal frequency range of these databases is constrained. The duration period is from 1 to 30 s The frequency range is below 195 Hz due to the low pass filter, which eliminates many essential heart sound characteristics for medical assessment. Furthermore, two of these databases are designed for the education of medical students. Consequently, they include high-quality records of strong murmurs that are typically not found in real-world recordings. Another factor is that the sensors or stethoscopes used by these datasets are expensive. Tables 2(a) and 2(b) show the comparison of collected datasets with other Online datasets. It gives detailed insight if the kind of dataset is available online the number of subjects, from which particular side the recordings were taken, what was the duration of the signal etc.

Table 2(a)
Comparison of collected dataset with other online datasets.

Database	Subject			
	Type	Number	Age	Gender
Physionet [13]	Normal Abnormal	Not provided	Not provided	Male Female
MHSD [13]	Normal (N) Pathological (P)	Not provided	Not provided	Not provided
PASCAL [14]	Normal Murmur Extra heart sound artifact Extrasystole	Not provided	Not provided	Not provided
Self-collected	Normal Abnormal murmurs	231 230	3–66 8–80	Male Female

Table 2(b)
Comparison of collected dataset with other online datasets.

Database	Recording					Sensor	
	Position/Area	State	Length (s)	Amount	Sampling frequency	Name	Frequency bandwidth
Physionet [13]	9 different positions	Rest	5–120	3126	4 kHz	Meditron electronic stethoscope	20–20 kHz
MHSD [13]	Apex aortic Pulmonic	Supine	Total: 1496.8 s	23	44.1 kHz	Stethoscope	Not provided
PASCAL [14]	Not provided	Not provided	1–30	176 (segmentation) 656 (classification)	4kHz	iStethoscope Pro iPhone app DigiScope	20 Hz to 20 kHz 20–1000 Hz
Self collected	Multi-position at chest	Rest Sitting Supine Sleeping	60 s	N: 2310 AM: 2300 Total: 4610	8 kHz	Self-designed DS-101	0–20 kHz

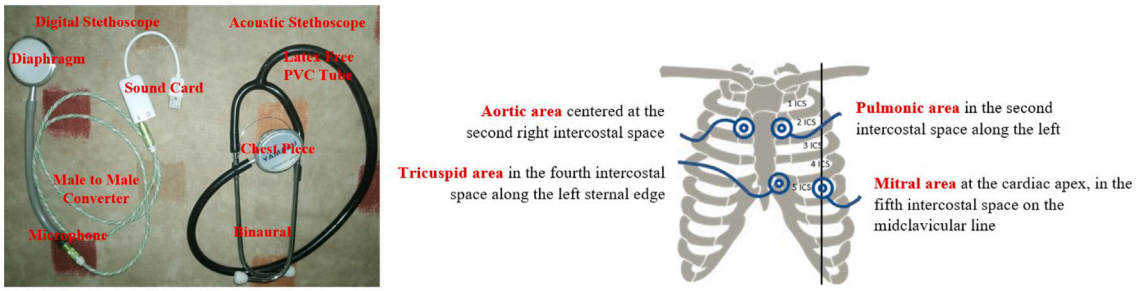

(a) (b)

Fig. 2. (a) Self-designed PCG acquisition system (b) Acquisition areas.

3.2. Self-collected database

We designed a real-time and low-cost PCG acquisition system to acquire PCG signals whose block diagram is shown in Fig. 1. A stethoscope chest piece (SCP) embedded with a microphone is placed above the chest near the heart region [8,14]. Fig. 2(a) shows the PCG acquisition setup, where an SCP is used to amplify and transmit the heart signal to a microphone, and Fig. 2(b) shows the areas from where the signals were acquired. The sounds in the heart are collected on the PC using a soundcard. The samples were labeled by an experienced cardiologist who tested each participant using medical methods. The sampling frequency is 8 kHz, and the signal is 10–60 s long for each PCG signal. This PCG data is obtained from several local and nearby hospitals, clinics, and nonclinical settings, such as in-home visits throughout 5 to 6 months during the daytime and evening. Major areas for data collection were Wah Cantt, Taxila, Rawalpindi, Hattar, Hassan abdal, Islamabad, and Lahore. Dataset was collected from normal and pathological children and adults (male and female). PCG signals were collected from aortic, pulmonic area, and tricuspid chest locations. The recordings include clear and pure heart sounds, but some recordings have overlapping respiration sounds and gastral

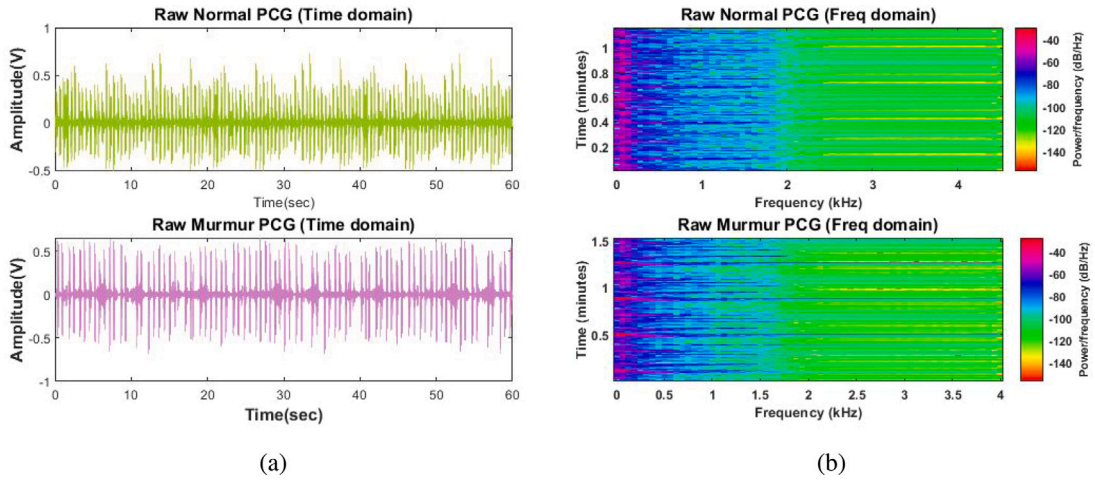

Fig. 3. (a) Raw signal in time domain (b) Raw signal in frequency domain.

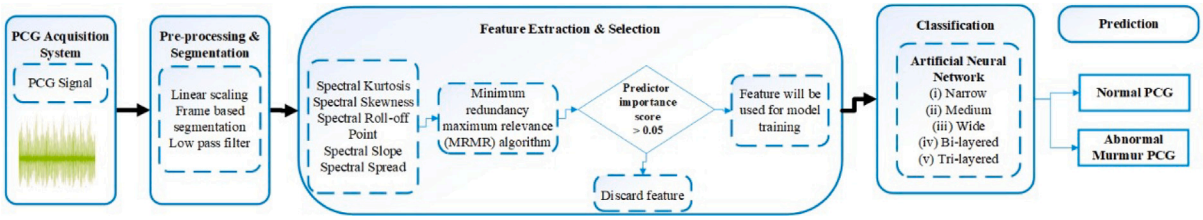

Fig. 4. Block diagram of proposed methodology.

Table 3
Dataset statistics.

Normal PCG			
Gender	Statistics		
	Subjects	Samples	Age
Male	115	1150	3–35
Female	116	1160	8–40
Total	231	2310	3–40
Abnormal murmur PCG			
Gender	Statistics		
	Subjects	Samples	Age
Male	111	1110	8–66
Female	119	1190	25–80
Total	230	2300	8–80

movements. This adds credibility to the collected dataset because if this dataset is used for real-time detection and classification of CVDs, any unseen PCG recording having lung, muscle, or gastral sound will still be correctly classified by the trained algorithm.

Fig. 3(a) shows the raw signal in time domain and Fig. 3(b) depicts the raw signal in frequency domain. Table 3 shows that a total of 4690 recordings were collected from 80 persons, among which 2300 recordings were positively identified as CVDs by medical experts. These CVD patients had the following heart-related problems,

i. Adult, toddlers and children: Heart valve problems, valve calcification, and endocarditis.
ii. Infants: Congenital heart defects and structural problems of the heart.

3.3. Anonymization

The process of anonymization is to protect the identity of patients so that it cannot be linked to any such system that could identify the patient. During data collection, we ensured to provide the anonymized data for further processing.

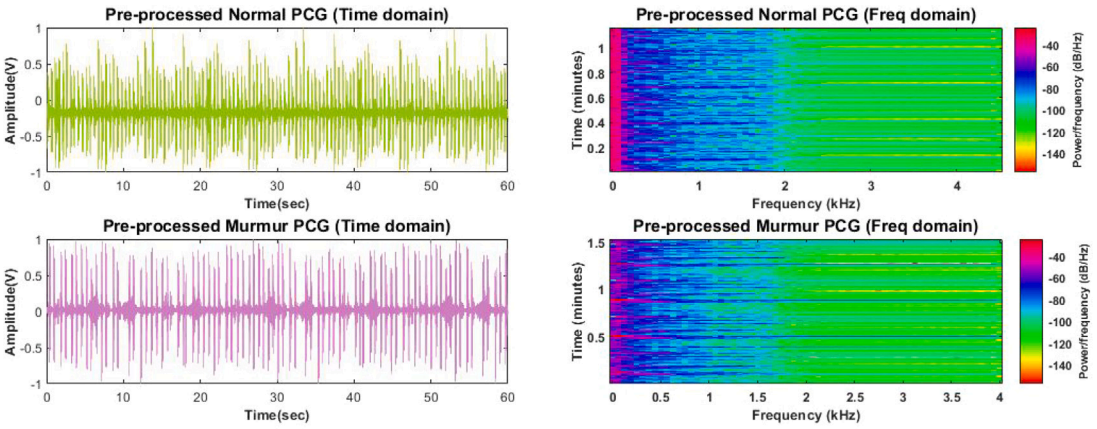

Fig. 5. (a) Pre-processed time domain signal (b) Pre-processed frequency domain signal.

4. Methodology

The methodology of the proposed system for the classification and detection of CVDs is shown in Fig. 4. The first step is to obtain the PCG signal through the heart of the subject/person/patient with the designed PAS. This raw PCG signal is then pre-processed by linear scaling, frame-based segmentation, and filtered by a low pass filter to remove high frequency components. The extracted spectral domain features are passed through a feature selection algorithm named minimum redundancy maximum relevance (MRMR). If the predictor importance score is greater than 0.05, only the feature is selected for model training. Eventually, five different types of ANN classifiers were successfully trained with high accuracy, sensitivity, and specificity to differentiate normal and abnormal heart murmurs.

4.1. Raw signal

The raw signal obtained from the PAS shows amplitude variation in the time domain as shown in Fig. 5(a). Raw normal PCG (RNP) signal range in amplitude varies from [1–0.5] while that of raw murmur PCG (RMP) signal is from [0.5–1]. RNP's frequency spectrum is from 0–2 kHz while RMP varies from 0–1.5 kHz as shown in Fig. 5(b). The color bar shows the energy content, meaning which frequency has what energy level, −40 dB/Hz is the highest energy content, while below −140 dB/Hz is the lowest. RNP contains heart sound, gastral, and muscle sounds, while RMP contains heart, respiration, and gastral sounds.

4.2. Pre-processing

The acquired PCG signal can have some noise created either due to wire resistance, inhale and exhale sounds during respiration, or sometimes it can also contain gastral reflex sounds. These components may lead to excluding valuable information that can help us differentiate CVDs. If this happens, then it complicates the classification method. To separate the rasping, whooshing, or blowing sounds created by the heart in PCG signals from respiration, lungs, gastral/bowel sounds, pre-processing, segmentation, and filtration are much-needed steps.

(1) Linear scaling

Mathematically Eq. (1)

$$Lin_{scPCGs} = \frac{P_{CGr} - Min_{PCGr}}{Max_{PCGr} - Min_{PCGr}} \tag{1}$$

where $PCGr$ is the raw signal obtained from sensor, **Min(PCGr)** is the minimum value present in PGS data and **Max(PCGr)** is the maximum value. As shown in Fig. 4, the amplitude range of both pre-processed PCG signals is [-1 1] in the time domain. The frequency plot shows that now both signals contain energy that is bundled. If we see Fig. 3(b) its energy was scattered, but Fig. 5(b) shows that now the energy content over frequency is more prominent, which helps us in analysis and experimentation.

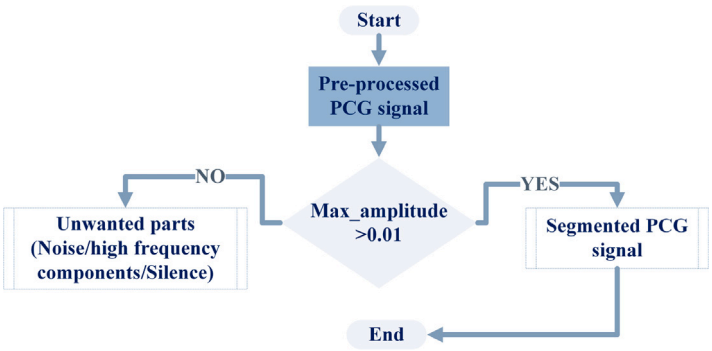

Fig. 6. Block diagram of Amplitude based segmentation.

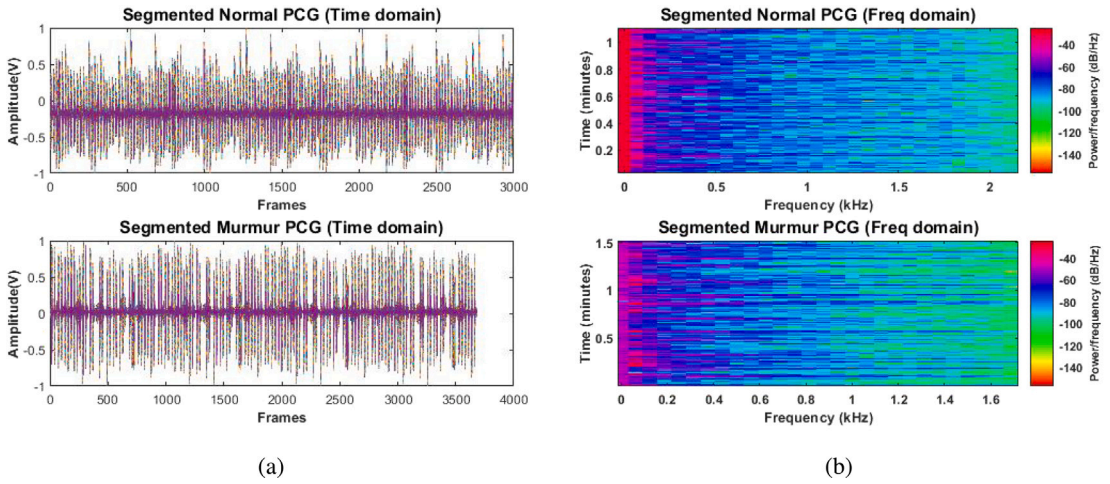

Fig. 7. (a) Time domain segmented signal (b) Frequency domain segmented signal.

4.3. Segmentation

Segmentation is done by framing, which partitions the PCG signal into smaller sections or slices. These signals are sectioned into 500 ms frames, with an overlap of 100 ms to remove the non-beating, high frequency, and any silent parts, if present. If a particular part of these smaller segments has an amplitude of less than 0.01, they will be removed, and all greater than it will be passed. This threshold value was selected after extensive visual analysis. The PCG signal contains the sound of closing and opening of cardiac valves, which is strongly audible, leading them to have higher and more prominent amplitudes while overlapping lung respiration and gastral reflexes (very few times) audible as background sounds with lower amplitudes. The block diagram of amplitude-based segmentation is shown in Fig. 6. Fig. 7(a) shows all the segments of normal and abnormal PCG signal in time domain while Fig. 7(b) shows the frequency representation. The segmented signal only contains that frequency content whose amplitude was greater than the 0.01 threshold. The segmented signal of Normal PCG contains prominent energy content from 0–2 kHz, while abnormal PCG signals contain 0–1.6 kHz.

4.4. Removal of high frequency components

A low-pass filter (LPF) only passes frequencies within a given spectrum and suppresses frequencies outside that range. Here, LPF is designed with a cut-off frequency of 250 Hz for a 3 dB point below the bandpass value. Because the range of heart sound only contains very low-frequency components, lub sound ranges from 40 to 200 Hz while dub sound from 50 to 250 Hz [15]. The frequency range of lung/respiration sounds ranges from 250- to 2k Hz [16] and bowel/gastral sounds up to 1500 Hz [17]. For a PCG signal, these sounds are high frequency components that add noise because any sound that is not produced by the heart in a PCG signal will be a noise element. Fig. 8 (a) is showing the filtered signal in time domain and Fig. 8(b) gives us the insight that both normal and abnormal signals contain frequency components that are lower than 250 Hz, which is the region of interest here. Normal PCG signals contain significantly lower frequency with prominent energy in 0–250 Hz, while abnormal murmur contains 0–100 Hz. Thus, we can now say that all raw PCG signals are filtered without any muscle, gastral, and respiration sounds.

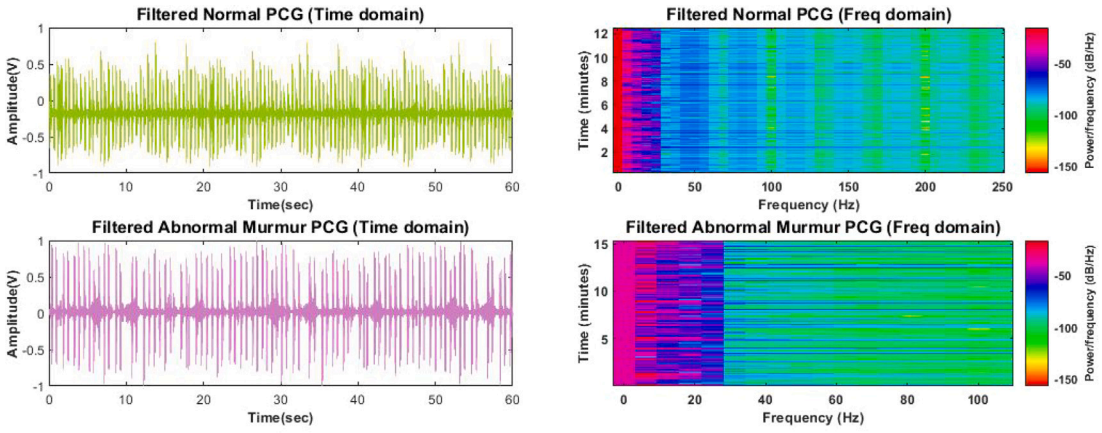

(a) (b)

Fig. 8. (a) Time domain filtered signal (b) Frequency domain filtered signal.

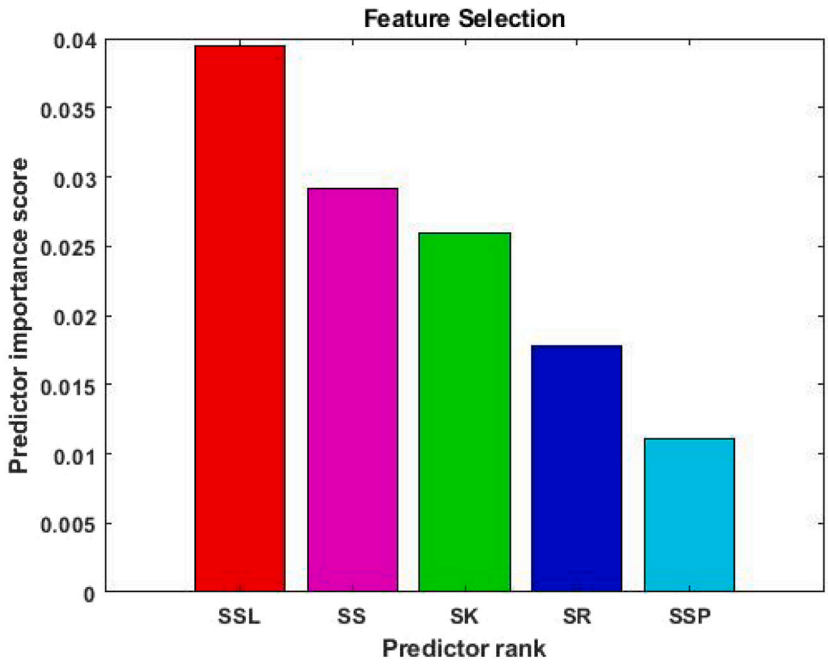

Fig. 9. Importance scores of extracted features obtained by MRMR algorithm.

4.5. Feature extraction and selection

Feature extraction is a method for extracting knowledge regarding signal functionality. It is also known as a function or features variable [18,19]. The spectral features mentioned below were extracted from filtered PCG signals. These feature vectors provide critical knowledge that aids identification using machine/deep learning methods. Thus, before model training, we tried to determine whether they would work or not by using the feature selection algorithm known as the minimum redundancy maximum relevance (MRMR) algorithm. The primary concept is that minimum redundancy must complement a maximum relevance condition for features that contribute to any particular class variable. We can say the global importance of the variables for the class is measured here [20]. Fig. 9 shows the MRMR of the extracted spectral features. The importance rank of variables for classification is given below.

Spectral Slope (SSL) > Spectral Skewness (SS) > Spectral Kurtosis (SK) > Spectral Rolloff Point (SR) > Spectral Spread (SSP)

As the importance scores of all the features are greater than 0.005, they will be able to perform excellent classification Fig. 9.

(1) Spectral kurtosis

SK can detect a series of transients as well as their frequency domain placements, and it can completely delete non-stationary data.

$$SK = \frac{\sum_{K=BE_1}^{BE_2} \left(f_k - Sc_1\right) S_k}{Sc_2 \sum_{K=BE_1}^{BE_2} S_k} \tag{2}$$

where $\boldsymbol{BE}$ represents band edges, $\boldsymbol{f_k}$ frequency bins, $\boldsymbol{S_k}$ Spectral values and $\boldsymbol{Sc}$ Spectral centroids.

Algorithm 1:SK

Input: F_{PCG}
Output: SK
for
  Find SC from F_{PCG}
  $\forall k$ *find* f_k
  Calculate BE_1 & BE_2
  $\forall k$ *find* s_k
  At bin k find spectral values (sk).
  SK= CUMSUM(SC1 $-$ fk)$_{BE2}^{BE1}$ *s_k
end

For spectral kurtosis calculation, convert and validate input filtered signal from the time domain to the spectral domain. Calculate centroids by taking the sum of frequency vectors and dividing them by filtered signal. Calculate band edges one ($\boldsymbol{BE_1}$) and two ($\boldsymbol{BE_2}$) respectively, and then spectral spread by taking the square root of the centroids sum and dividing the sum by filtered signal **(see Algorithm 1)**.

(2) Spectral skewness

Spectral Skewness represents the sum of variation in the spectrum shape between the occurrences above the normal frequency but under the center of mass.

$$SS = \frac{\sum_{K=BE_1}^{BE_2} \left(f_k - Sc_1\right)^3 \; S_k}{SS\, 2 \sum_{K=BE_1}^{BE_2} S_k} \tag{3}$$

where $\boldsymbol{BE}$ represents band edges, $\boldsymbol{f_k}$ frequency bins, $\boldsymbol{S_k}$ spectral values, $\boldsymbol{SS}$ spectral spread and $\boldsymbol{Sc}$ spectral centroids.

Algorithm 2:SS

Input: F_{PCG}
Output: SS
for
  Convert and validate F_{PCG} from a T_d to S_d.
  Calculate S_c by $\frac{FV^2}{S_{d-PCG}}$ and BE_1 and BE_2.
  Calculate SS by taking $\sqrt{\frac{{S_c}^2}{{F_{PCG}}^2}}$
end

To calculate SS ID- filtered heart PCG is converted from a time domain to spectral domain signal. Its centroids are calculated by taking the sum of frequency vectors and dividing them by filtered PCG. Calculate band edges and finally get the value of SS by taking the square root of the sum of centroids and dividing by the sum of an input signal **(see Algorithm 2)**.

(3) Spectral roll-off point

SR is a frequency domain parameter that gives information about a frequency below which a particular amount of spectral energy is dissipated. [21].

$SR = i$

$$\sum_{K=BE_1}^{i} S_{K=TE} \sum_{K=BE_1}^{BE_2} S_k \tag{4}$$

where ***BE*** represents band edges, f_k frequency bins, S_k spectral values and ***Sc*** spectral centroids.

Algorithm 3:SR

Input: F_{PCG}
Output: SR
for
  Calculate TH_s.
  Find PS of F_{PCG} by converting it T_d.
  CUMSUM S_{d-PCG} * TH_s.
  FV=ids > TH_s.
  Reshape FV according to F_{PCG} channels.
end

Find a specified threshold for input filtered signal, convert this time series data to the power spectrum and then calculate the cumulative sum of the signal and multiply it with a threshold. Find the ids greater than the chosen threshold, save them in a frequency vector and reshape them according to input channels **(see Algorithm 3)**.

(4) Spectral slope

SSL is a linear regression-based estimate of the audio signal's rapid transition to higher frequencies. Many normal audio signals have a spectral pitch that is lower in frequency and higher in frequency. The quality of the acoustic signals is responsible for this slope. SSL generates a single numerical value representing the direction of the best match line based on spectral performance.

$$SSL = \sum_{K=BE_1}^{BE_2} (f_K - MF) \frac{(f_K - MF)(f_K - MS)S_K}{\sum_{K=BE_1}^{BE_2} (f_K - MF)^2} \tag{5}$$

where ***BE*** represents band edges, f_k frequency bins, S_k spectral bin values, ***MF*** is mean frequency and ***MS*** is mean value of spectra.

Algorithm 4:SSL

Input: F_{PCG}
Output: SSL
for
  Convert F_{PCG} from a T_d to S_d.
  V= $\frac{Total_{freq} - Ch_{1\_freq}{}^2}{F_{PCG}}$
  RV=F_{PCG}- $Ch_1{}^2$
  Reshape (RV_{ch})
end

Convert filtered signal from a time domain to spectral domain, subtract total frequency from the sum of frequencies of channel one and divide them by the filtered signal. Apply element-wise minus binary operation to filtered signal and sum of amplitude of channel one while enabling the implicit expansion and reshaping the returned value according to input channels **(see Algorithm 4)**.

(5) Spectral spread

It is also associated with the signal bandwidth and is the mean rate map variation around the center. Noise-like signals are generally of high spectral distribution, although isolated tones tend to be low spectral distribution.

$$SSP = \sqrt{\frac{\sum_{K=BE_1}^{BE_2} (f_K - Sc_1)S_K}{\sum_{K=BE_1}^{BE_2} S_K}} \tag{6}$$

where ***Sc*** spectral centroids, f_k frequency bins, S_k spectral bin values and ***BE*** represents band edges.

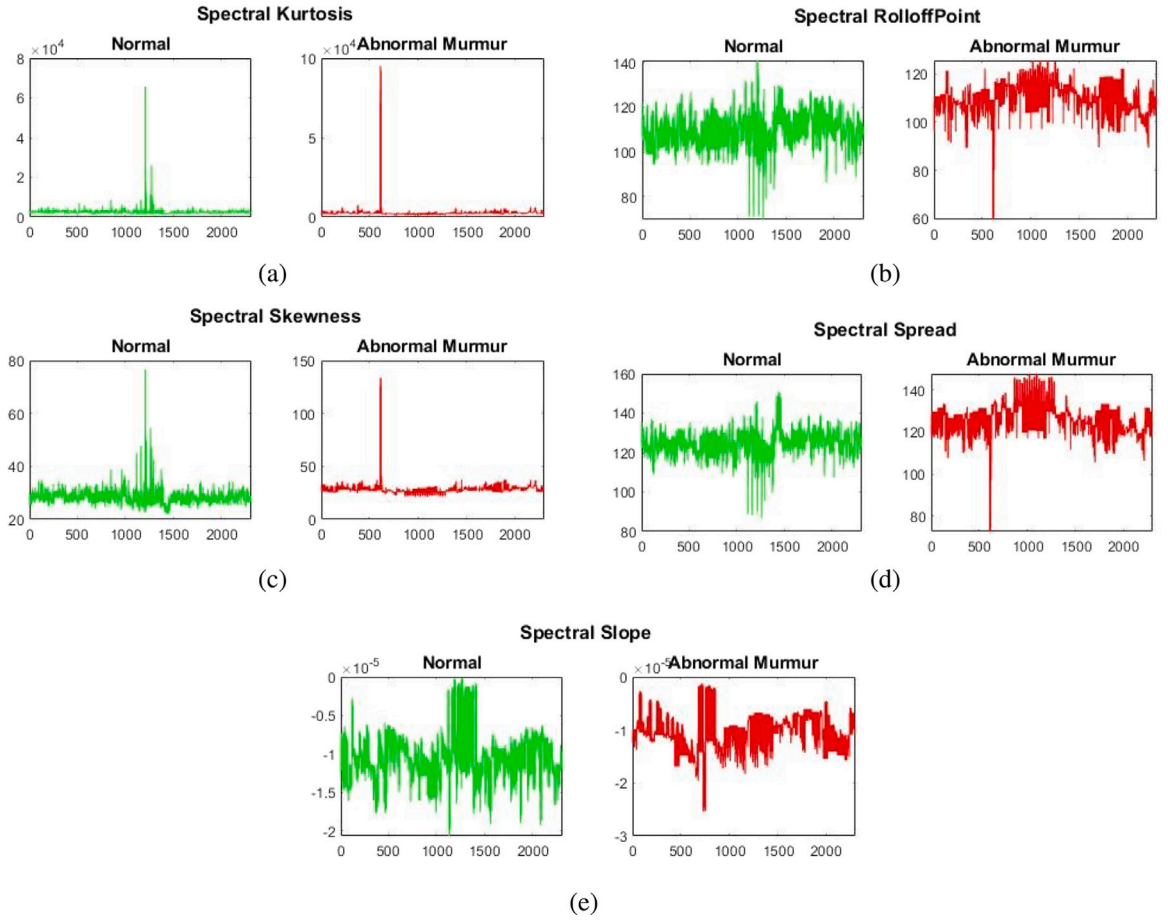

Fig. 10. 2D plots of (a) Spectral kurtosis (b) Spectral rolloffpoint (c) Spectral skewness (d) Spectral spread (e) Spectral slope.

Algorithm 5:SSP

Input: F_{PCG}
Output: SSP
for
  Convert F_{PCG} from a T_d to S_d.
  $C_n = (F_{PCG} + FV)_{ij}$
  $SSP = (C_n + FV)_{ij}$
  Reshape (SSP).
end

Convert filtered signal from a time domain to spectral domain and calculate centroids by applying element-wise time over signal and frequency vectors. Find spectral spread by applying element-wise binary operation over frequency vectors and calculated centroids. Reshape the acquired values according to the number of input channels **(see Algorithm 5)**. The 2-D plots of all the extracted spectral features are shown in Fig. 10(a)–(e).

4.6. Classification

Classification is described as a machine learning and statistics-based supervised learning approach. In it, a computer program learns from data and generates new observations or classifications. This is the complete process of classifying a collection of raw or pre-processed data.

A neural network is a collection of neurons grouped to form a cutting-edge perspective. A neural arrangement is a natural neural structure composed of discrete neurons or a man-made neural architecture designed to deal with man-made brainpower

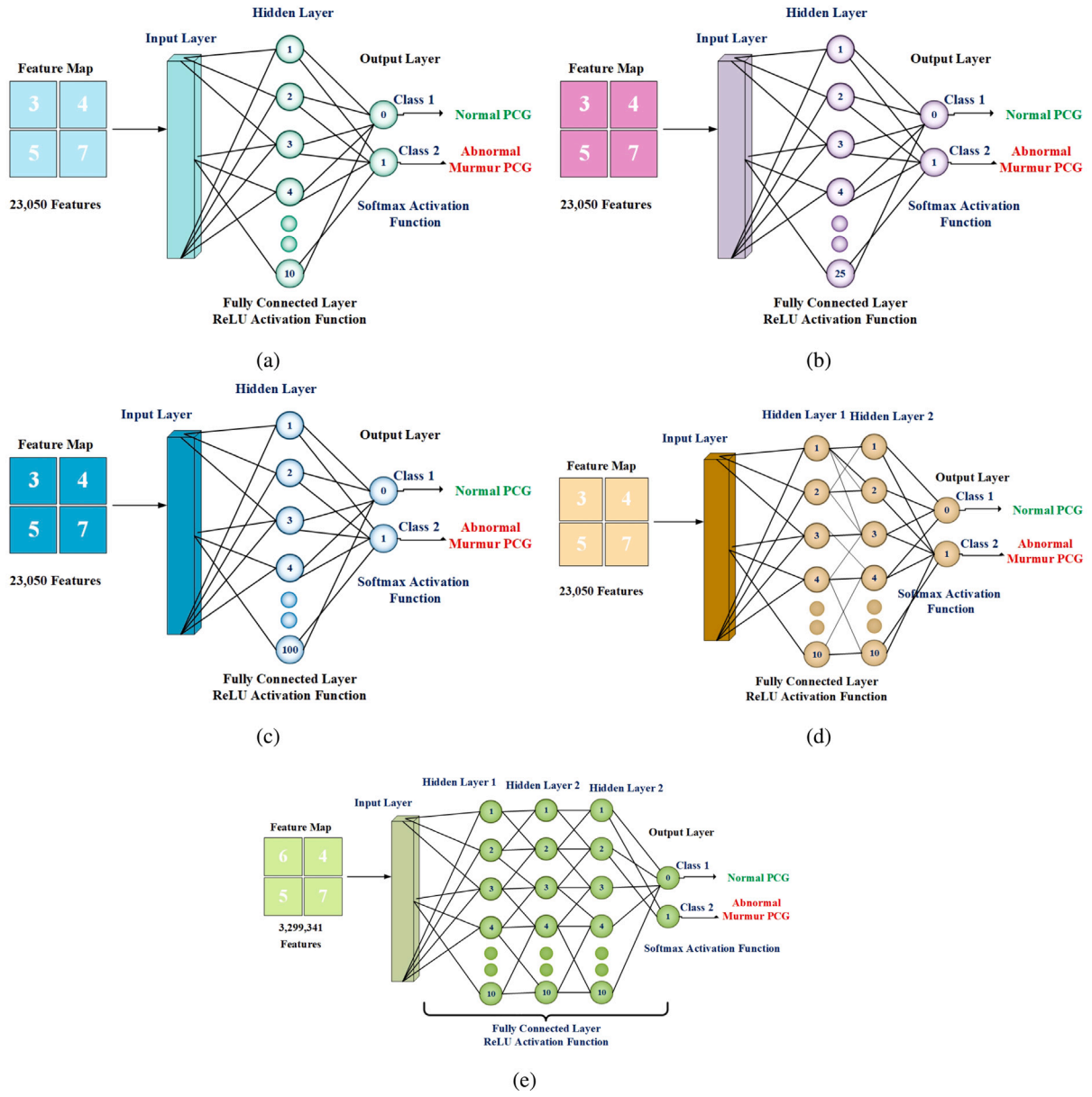

Fig. 11. Architecture of artificial neural network (a) Narrow (b) Medium (c) Wide (d) Bi-layered (e) Tri-layered.

Table 4
Parameters of different types of neural networks.

Neural network type	Number of fully connected layers	Layer size	Activation	Iteration limit	Standardize data
Narrow	1	First: 10	ReLU	1000	Yes
Medium	1	First: 25	ReLU	1000	Yes
Wide	1	First: 100	ReLU	1000	Yes
Bilayered	2	First: 10 Second:10	ReLU	1000	Yes
Trilayered	3	First: 10 Second:10 Third:10	ReLU	1000	Yes

difficulties [22]. They mirror the conduct of the human cerebrum, permitting computers to perceive designs and take care of normal issues in the fields of computer-based intelligence, AI, and profound learning. Neural networks, also known as artificial neural networks are a field of artificial intelligence (AI) that is the heart of deep learning algorithms. The human cerebrum inspired their name and design, which is modeled on how organic neurons interact with one another.

Neural Networks are multi-input, multi-output systems made up of artificial neurons. Every neuron impacts one another, as they are associated. The main objective of a neural network is to translate input into a distinct value. The organization can recognize and notice each part of the current dataset and how the various pieces of information might identify one another. This is how neural networks are equipped to discover amazingly complex examples in immense volumes of information.

Here we used 5 different types of artificial neural network classifiers named narrow neural network (NNN), medium neural network (MNN), wide neural network (WNN), bilayered neural network (BNN), trilayered neural network (TNN) to train extracted features. An ANN contains 3 layers, as shown in Fig. 11(a)–(e) and Table 4 shows the detailed architecture and inside information.

4.6.1. Input layer

Flatten is the operation that transforms the pooled features maps into a single column sent to the fully linked layer. Here, we are transforming the input data into a 1-dimensional array. The extracted spectral features from PCG signals are flattened to form a single long feature vector, then fed into hidden neural network layers for further processing. Mathematically,

$$Before\ flattening = \begin{bmatrix} 1 & \cdots & 0.7 \\ 5.66 & \cdots & 8.9 \\ 9.99 & \cdots & 3.3 \end{bmatrix} \tag{7}$$

$$After\ flattening = \begin{bmatrix} 1 \\ \cdots \\ 0.7 \\ 5.66 \\ \cdots \\ 8.9 \\ 9.99 \\ \cdots \\ 3.3 \end{bmatrix} \tag{8}$$

4.6.2. Hidden layers

The hidden layer is positioned between the algorithm's input and output, in which the function applies weights to the inputs and guides them through an activation function as the output. Mathematically,

$$O_n = \varphi(\sum_i w_{cc} n_i + b_n) \tag{9}$$

where n_i represents each neuron's set of inputs, O_n is each neuron's set of outputs, and b_n is each neuron's bias set. A weight coefficient, w_{cc}, is applied to each input, and the activation function is represented by φ.

4.6.3. Activation Function (AF)

Here rectified linear activation unit (ReLU) has been used as an AF. This function increases the sensitivity of the activation sum input while preventing saturation. It is a piecewise linear function that will output the input directly if it is positive and zero otherwise. It was chosen because it solves the problem of vanishing gradients, enabling NN to train quicker and function effectively. Mathematically,

$$f(x) = max(0, x) \tag{10}$$

4.6.4. Output layer

The output layer of an ANN is the final layer of neurons that generates the program's outputs. For binary classification of PCG signal, we modified the last layer to 2 as we have only two classes, normal and abnormal murmur PCG.

$$Neuron_{out} = F\left(w_1 x_1 + w_2 x_2 + b\right) \tag{11}$$

The above network takes numerical inputs x_1, x_2 which has weights w_1 and w_2, a bias b and activation function F.

5. Results and discussions

CVDs can be classified by using analysis, different signal processing algorithms, and an automatic screening process. This proposed methodology used pre-processing, segmentation, feature extraction, and classification processes to minimize the prediction time used during the overall procedure. It achieved a cumulative accuracy of 99.9 percent for normal and abnormal cardiac PCG signals. The proposed algorithm yields an efficient and fast PCG classification with better discriminating results. The primary goal was to create an intelligent PCG algorithm for cardiac disease.

Table 5
Features analysis.

Features	Normal PCG			
	Min	Max	Standard deviation	Mean
SK	$1.3715e^{3}$	65 664	$1.6729e^{3}$	$2.5582e^{3}$
SS	22.0050	76.6800	2.7803	28.2121
SR	69.6970	140.9700	7.8661	110.3320
SSL	$-2.0635e^{-5}$	$-1.8164e^{-7}$	$3.6739e^{-6}$	$-1.0417e^{-5}$
SSP	86.7450	150.6000	6.6215	125.7255
Features	Abnormal murmur PCG			
	Min	Max	Standard deviation	Mean
SK	$1.2035e^{3}$	95 206	$4.9701e^{3}$	$2.9924e^{3}$
SS	21.5110	133.5400	6.8164	29.0891
SR	59.6860	125.5100	7.6880	108.6853
SSL	$-2.5385e^{-5}$	$-1.2752e^{-6}$	$3.9799e^{-6}$	$-1.0452e^{-5}$
SSP	72.6110	147.6500	9.0658	124.6915

5.1. Clinical relevance

Clinically, the proposed study ensures that cardiac PCG diseases based on PCG signals are appropriately classified. Unlike the traditional stethoscope, which is used to diagnose diseases manually, PCG acquisition system combined with a neural network-based prediction model reduces manual disease detection errors. This can positively help clinicians with clinical decisions resulting in early detection. Furthermore, while manual diagnosis and chest x-rays may result in a correct diagnosis, it is still highly recommended to build an automatic system that identifies abnormalities in patients with non-invasive and non-radiative technologies. These intelligent, on-invasive systems will significantly improve diagnostics and function as supportive decision-makers in real-time clinical situations.

5.2. Feature analysis

Here we performed feature analysis through descriptive statistics, which contain min, max, standard deviation, and mean as shown in Table 5.

1. **Standard Deviation (SD)** is a representation of how the data is distributed about the average. The standard deviation of SS, SR, SSP are slightly higher, showing that these data points are slightly above the average. SSL has a low standard deviation (LSD) which suggests that the data is grouped around the mean and SK has the highest standard deviation (HSD), meaning that data is dispersed.
2. The **minimum and maximum numbers** determine the total range of our data. SSL contains the lowest min among all features, while SK has the highest max.
3. The **mean value** is significant because it indicates where the dataset's center value is based. It also includes information from each sample in a dataset, but it can be false if the data source is skewed or contains outliers. This is the value with the smallest margin of error. SK has the highest mean, while SSL has the lowest mean value.

5.3. Performance analysis

Detailed performance analysis of each classifier is done by using accuracy (AC), sensitivity (SN), specificity (SP), precision (PR), f1-score (FS), and Matthew's correlation coefficient (MCC) [21,22].

1. **Narrow Neural Network**
   The lowest accuracy (90%) is achieved by training NNN on spectral skewness, training NNN achieves the lowest sensitivity (90.87%) on spectral roll-offpoint, spectral skewness, achieves the lowest specificity of (87.14%), lowest precision and MCC of (86.09%) and (80.24%) is also achieved by spectral skewness. The best accuracy, sensitivity, specificity, precision, f1-score, and MCC score of (99.99%) is achieved by training NNN on spectral spread and when all combined (SK+SS+SR+SSL+SSP) features are used.
2. **Medium Neural Network**
   The lowest accuracy (90.65%), specificity (88.21%), precision (87.39%), f1-score (90.32%), and MCC (81.47%) is achieved by Spectral skewness while spectral roll-offpoint achieves the lowest sensitivity (91.72%). The best accuracy, sensitivity, specificity, precision, f1-score, and MCC score of 99.99% is achieved by training MNN on spectral slope, spectral spread, and when combined, (SK+SS+SR+SSL+SSP) features are used.

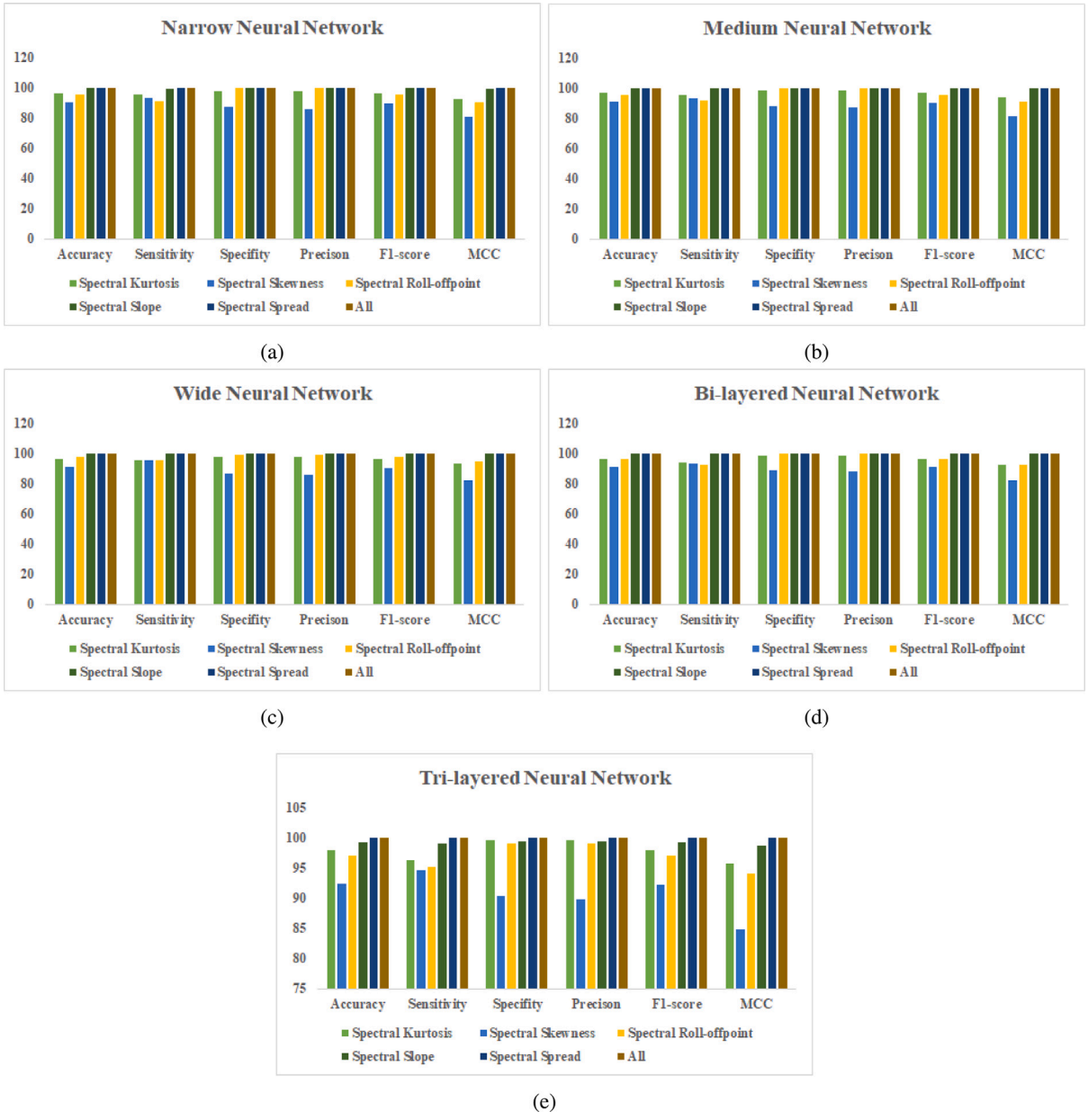

Fig. 12. Performance comparison of ANN with different feature combinations (a) NNN (b) MNN (c) WNN (d) BNN (e) TNN.

3. **Wide Neural Network**
   The lowest accuracy (90.72%), specificity (86.84%), precision (85.39%), f1-score (90.17%), and MCC (81.89%) is achieved by spectral skewness while spectral kurtosis achieves the lowest sensitivity (95.1%). The best accuracy, sensitivity, specificity, precision, f1-score, and MCC score of 99.99% is achieved by training MNN on spectral slope, spectral spread, and when combined, (SK+SS+SR+SSL+SSP) features are used.
4. **Bi-layered Neural Network**
   The lowest accuracy (90.89%), specificity (88.6%), precision (87.87%), f1-score (90.59%), and MCC (81.92%) is achieved by spectral skewness while spectral roll-offpoint achieves the lowest sensitivity (92.63%). The best accuracy, sensitivity, specificity, precision, f1-score, and MCC score of 99.99% is achieved by training BNN on spectral slope, spectral spread, and all combined (SK+SS+SR+SSL+SSP) features are used. spectral roll-offpoint-BNN also achieves 99.99% specificity and precision.

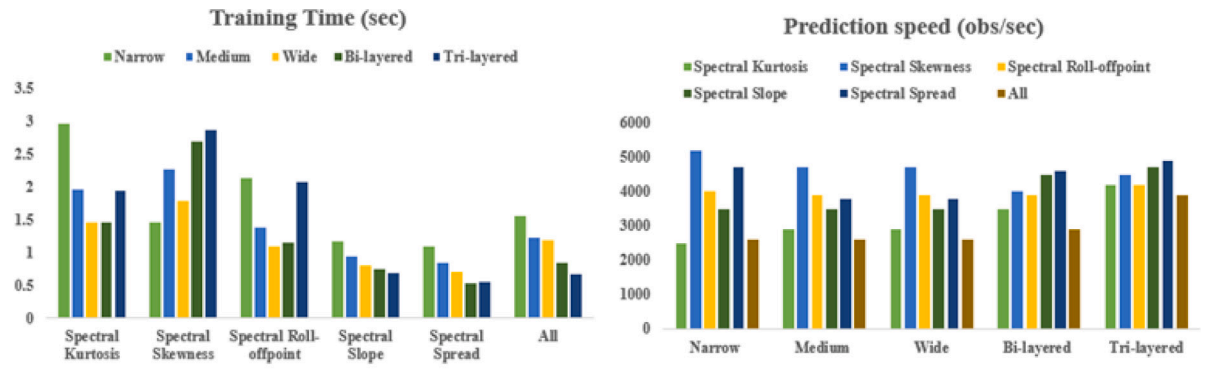

Fig. 13. Timing Analysis (a) Training Time (b) Prediction Speed (Testing phase).

5. **Tri-layered Neural Network**
   The lowest accuracy (92.36%), sensitivity (94.68%), specificity (90.29%), precision (89.74%), f1-score (92.14%) and MCC (84.84%) is achieved by spectral skewness. The best accuracy, sensitivity, specificity, precision, F1-score, and MCC score of 99.99% is achieved by training TNN on spectral spread and when all combined (SK+SS+SR+SSL+SSP) features are used.

Thus, it can be said that to achieve the best results, all combined features or spectral spread must be used to train the neural networks as it will help us classify the CVD's with high sensitivity and specificity.

By using above parameters, we also performed an extensive performance analysis of whole algorithm on multiple conditions. Fig. 12(a)–(e) shows a detailed comparison of accuracy, sensitivity, specificity, precision, f1-score and matthew's correlation coefficient. Mathematically,

$$AC = \frac{(TP + TN)}{(TP + TN + FP + FN)} \tag{12}$$

$$SN = \frac{TP}{TP + FN} \tag{13}$$

$$SP = \frac{TN}{TN + FP} \tag{14}$$

$$FS = \frac{2 * TP}{(2TP + FP + FN)} \tag{15}$$

$$MCC = \frac{TP * TN - FP * FN}{\sqrt{((TP + FP) * (TP + FN) * (TN + FP) * (TN + FN))}} \tag{16}$$

The individual features spectral spread, and spectral slope achieved the highest accuracy (99.9%), precision (99.9%), f1-score (99.9%) on medium, wide, narrow, bi-layered, and tri-layered NN.

5.4. Timing and speed analysis

NNN-SS combination took only 1.0844 s to train the whole dataset, MNN-SS took 0.83335 s, WNN-SS took 0.70847 s, BNN-SS took 0.53932 s, and TNN-SS took 0.5514 s Spectral skewness combination with NNN during the testing phase was predicted at the rate of 5200 observations per second. With MNN, it predicted 4700 observations per second. With WNN, it predicted 4600 observations per second. With BNN, it predicted 5500 observations per second. With MNN, it predicted 4900 observations per second. Thus, Spectral skewness timing performance is best among all other extracted features.Fig. 13(a) gives the insight of training time taken by all the models and Fig. 13(b) tells us the time it took each classifier to predict on the unseen test dataset.

5.5. Comparative analysis

The proposed approach performs better than the existing approaches because spectral features uncover that information that would remain hidden in time, statistical and impulsive domains. The amount of collected datasets is also substantial for binary classification. Also, pre-processing steps excellently purified the PCG signal such that only low-frequency heart components are present. As neural network techniques perform 31% better than machine learning methods for classification purposes, the use of five different types of ANN helped us achieve the best accuracy, sensitivity, specificity, and f1 scores. Table 6 gives us a detailed comparison of the proposed methodology with the state-of-the-art methods.

Table 6
Comparison of proposed methodology with the state-of-the-art methods.

Reference	Signal used/Classes	Pre-processing	Feature extraction	Classifier	Classification merit	Limitations
[6]	PCG Normal vs. Abnormal	Downsampling Filter and segmentation: Wavelet analysis	Normalized average Shannon energy	AR model	SN: 87% SP: 61% FS: 74%	Classification accuracy is not high. The parameters threshold setting is selected by experiment experience.
[7]	PCG S1 vs. S2	Decomposition into AM-FM signal Linear low-pass filter	Shannon energy	Hidden Markov model (HMM)	SN of S1: 98.6% SN of S2: 98.3%	Due to the homomorphic filtering, there are deviations between the envelogram peak and the maximum absolute value of the original peak.
[8]	PCG Normal vs. Extrahls	Empirical mode decomposition Soft thresholding based signal segmentation	Impulsive domain features	Ensemble classifier	AC: 98.8%, SP: 97.56% SN: 99.99%	Amount of collected dataset is small.
Proposed methodology	PCG Normal vs. Abnormal murmur	Normalization segmentation Low pass filter	Spectral features	Five different types of artificial neural network	AC: 99.9% SN: 99.9% SP: 99.9% PR: 99.9% FS: 99.9% MCC: 99.9%	

6. Conclusion

Pre-processing and classification of cardiac sounds are difficult because of environmental and overlapping muscle sounds. To address the mortality caused by CVDs, an effective method for the detection and classification of normal and abnormal heart murmurs with the help of PCG signals is discussed here. Dataset is acquired from a local hospital with the help of a self-designed sensor. A total of 4610 samples are collected with a sampling frequency of 44.1 kHz. Raw PCG signals are pre-processed and segmented by linear scaling (LS), framing, and low pass filter. LS removes variation, segmentation removes noise/silence parts, while a low-pass filter removes high-frequency components (>250 Hz). Extracted spectral features exhibit good discriminatory properties for classification when trained on neural networks. 5 different types of ANN were trained and tested on the dataset. The spectral spread feature achieved an accuracy of 99.99% and with a combination of all features combined, all ANN's achieved 99% accuracy. The PCG acquisition system designed is non-invasive and cheap but one of the shortcomings of this methodology is that here we are only doing binary classification of normal and abnormal murmurs, which does not give detailed insight. There must be a system that performs multi-class classification and tells the exact type of murmur like systolic, diastolic, and continuous murmur. Our work is also restricted in that it only examines a few neural network and feature extraction techniques. It might be feasible to improve the proposed model by experimenting with various ways; however, it is impossible to predict which would be useful without substantial testing and analysis. As the presented framework is independent of the morphological characteristics of raw PCG signals, that is why in the near future, we aim to apply feature fusion and feature reduction techniques for better accuracy performance.

Declaration of competing interest

The authors declare that they have no known competing financial interests or personal relationships that could have appeared to influence the work reported in this paper.

Acknowledgments

The researchers would like to thank University of Engineering and Technology, Taxila, Pakistan. This research was supported by Taif University Researchers Supporting Project number (TURSP-2020/126), Taif University, Taif, Saudi Arabia, Basic Science Research Program through the National Research Foundation of Korea(NRF) funded by the Ministry of Education (NRF-2021R1A6A1A03039493) and in part by the NRF grant funded by the Korea government, Ministry of Science and ICT (MSIT) (NRF-2022R1A2C1004401).

References

[1] Ma A. Digital subtraction phonocardiography (DSP) applied to the detection and characterization of heart murmurs. Biomed Eng Online 10. http://dx.doi.org/10.1186/1475-925X-10-109.
[2] Sundaram DSB, Shivaram S, Balasubramani R, Muthyala A, Arunachalam SP. Discriminating normal phonocardiogram from artifact using a multiscale entropy technique. In: IEEE int. conf. electro inf. technol, 2019-May. p. 542–5.
[3] Sarbandi RR, Doyle JD, Navidbakhsh M, Hassani K, Torabiyan H. A color spectrographic phonocardiography (CSP) applied to the detection and characterization of heart murmurs: Preliminary results. Biomed Eng Online 10.
[4] Liang H, Lukkarinen S, Hartimo I. Heart sound segmentation algorithm based on heart sound envelogram. Comput Cardiol 105–8.
[5] Huiying L, Sakari L, Iiro H. Heart sound segmentation algorithm using wavelet decomposition and reconstruction. In: Annu int. conf. IEEE eng. med. biol., proc., Vol. 4. p. 1630–3.
[6] He R, Zhang H, Wang K, Li Q, Sheng Z, Zhao N. Classification of heart sound signals based on AR model. Comput Cardiol 43:605–8.
[7] Gill D, Gavrieli N, Intrator N. Detection and identification of heart sounds using homomorphic envelogram and self-organizing probabilistic model. Comput Cardiol 32:957–60.
[8] Khan MU, Ali SZuriat-e-Zehra, Ishtiaq A, Habib K, Gul T, Samer A. Classification of multi-class cardiovascular disorders using ensemble classifier and impulsive domain analysis. Int Conf Comput 1–8.
[9] Choi S, Jiang Z. Cardiac sound murmurs classification with autoregressive spectral analysis and multi-support vector machine technique. Comput Biol Med 40(1):8–20.
[10] Banerjee M, Majhi S. Multi-class heart sounds classification using 2D-convolutional neural network. In: Proc. 2020 int. conf. comput. commun. secur. ICCCS 2020.
[11] Babaei S, Geranmayeh A. Heart sound reproduction based on neural network classification of cardiac valve disorders using wavelet transforms of PCG signals. Comput Biol Med 39(1):8–15.
[12] Ahmad MS, Mir J, Ullah MO, Shahid MLUR, Syed MA. An efficient heart murmur recognition and cardiovascular disorders classification system. Australas Phys Eng Sci Med 42(3):733–43.
[13] Liu C. An open access database for the evaluation of heart sound algorithms. Physiol Meas 37(12):2181.
[14] Challenge, classifying heart sounds. 2021, (accessed Sep. 18, 2021).
[15] Yaseen, Son GY, Kwon S. Classification of heart sound signal using multiple features. Appl Sci 8(12):2344.
[16] Naqvi SZH, Arooj M, Aziz S, Khan MU, Choudhary MA, Hassan MNUl. Spectral analysis of lungs sounds for classification of asthma and pneumonia wheezing. In: 2nd int. conf. electr. commun. comput. eng. ICECCE.
[17] Kölle K, Aftab MF, Andersson LE, Fougner AL, Stavdahl . Data driven filtering of bowel sounds using multivariate empirical mode decomposition. Biomed Eng Online 18(1):1–20.
[18] Tahir S. Extended Kalman filter-based power line interference canceller for electrocardiogram signal.
[19] Khan MU, Farman A, Rehman AU, Israr N, Ali MZH, Gulshan ZA. Automated system design for classification of chronic lung viruses using non-linear dynamic system features and K-nearest neighbour. Int Conf Comput 1–8.
[20] Acid S, De Campos LM, Fernández M. Minimum redundancy maximum relevancy versus score-based methods for learning Markov boundaries. Int Conf Intell Syst Des Appl ISDA 619–23.
[21] Tan L, Yu K, Bashir AK, Cheng X, Ming F, Zhao L, Zhou X. Toward real-time and efficient cardiovascular monitoring for COVID-19 patients by 5G-enabled wearable medical devices: a deep learning approach. In: Neural computing and applications. Springer.
[22] Ashraf I, Alnumay WS, Ali R, Hur S, Bashir AK, Zikria YB. Prediction models for COVID-19 integrating age groups, gender, and underlying conditions, Vol. 67. CMC- Computers, Materials & Continua; p. 3009–44.

Misha Urooj Khan is a Research Assistant at the National Center of Artificial Intelligence with a master's degree in Electronic System Design. She is the Chairperson of the Community of Research and Development (CRD). Her main research interests are machine learning, deep learning, audio processing, digital signal, and image processing with 25 publications regarding them.

Sana Samer is a student of BS Electronics Engineering at UET Taxila, Pakistan. Her research interests are electromyography, medical signal processing, and signal classification. Currently, she is working as an intern in Swarm Robotics Lab, Computer Engineering Department, UET Taxila and is a member of the Community of Research and Development (CRD).

Mohammad Dahman Alshehri is an Assistant Professor at Computer Science Department, Taif University, Saudi Arabia. He received his Ph.D. in Artificial Intelligence of Cybersecurity for the Internet of Things (IoT). He developed 6 smart novel algorithms for IoT to reinforcement Cybersecurity with AI. He has several publications in high-ranked international journals and top-tier conferences.

Hareem Khan is crew secretary of intelligent systems design at Community of Research and Development (CRD) and has done her B.Sc. degree in Computer Engineering from UET Taxila with a bronze medal. She is the AI head of Taxilian Robotics and Automation Club (TRAC) and has multiple publications. Her research interests are machine learning, digital logic design, and web designing.

Naveed Khan Baloch has published many research papers in his field and has experience in embedded system designing, fault-tolerant systems, and reconfigurable computing. Nowadays he is working as Assistant Professor in Computer Engineering Department at UET Taxila. During his tenure in academia, he did many collaborations with industry and foreign universities regarding on-chip networks, embedded vision, and reconfigurable computing.

Fawad Hussain is currently working as an Assistant Professor in the Computer Engineering Department, the University of Engineering and Technology (UET), Taxila, Pakistan. He received his bachelors, masters, and Ph.D. degree from University of Engineering and Technology (UET), Taxila, Pakistan in 2005, 2009, and 2015 respectively. His research interest includes network-on-chip, speech and audio processing, computer vision, and emotion recognition.

Sung Won Kim received his B.S. and M.S. degrees from the Department of Control and Instrumentation Engineering, Seoul National University, Korea, in 1990 and 1992, respectively, and his Ph.D. degree from the School of Electrical Engineering and Computer Sciences, Seoul National University, Korea, in August 2002. In March 2005, he joined the Department of Information and Communication Engineering, Yeungnam University, Gyeongsangbuk-do, Korea, where he is currently a Professor. His research interests include wireless networks.

Yousaf Bin Zikria (Senior Member, IEEE) is currently working as an Assistant Professor with the Department of Information and Communication Engineering, College of Engineering, Yeungnam University, Korea. His cumulative journal impact factor is more than 320. He has been listed in the world's top 2% researchers/scientists published by Elsevier and Stanford University.